RARE BEAUTY AND CHARM DECAYS AT LHCB

C. PARKINSON, on behalf of the LHCb collaboration
Imperial College London, South Kensington Campus, London SW7 2AZ, England

New results are presented using a data sample with an integrated luminosity of $\sim 1\,\text{fb}^{-1}$ collected in 2011 with the LHCb detector. The $B \to \mu^+\mu^-$ and $D^0 \to \mu^+\mu^-$ results have been presented at a previous conference. The angular distributions and (partial) branching fractions of selected radiative penguin decays are studied using a data sample with an integrated luminosity of $\sim 1\,\text{fb}^{-1}$ collected in 2011 with the LHCb detector. The partial branching fraction and theoretically clean observables of the decay $B^0 \to K^{*0}\mu^+\mu^-$ have been extracted as a function of the dimuon invariant mass. The partial branching fraction of the decay $B_s^0 \to \phi\mu^+\mu^-$ has also been extracted as a function of the dimuon invariant mass. The branching fraction and first observation of the decay $B^+ \to \pi^+\mu^+\mu^-$ is reported. New limits were set on the decay $B \to \mu^+\mu^-\mu^+\mu^-$. Improved limits on the decays $B \to \mu^+\mu^-$ and $D^0 \to \mu^+\mu^-$ are also presented.

1 Introduction

In the Standard Model (SM), B and D mesons can decay via Flavour-Changing Neutral Current (FCNC) processes mediated by loop diagrams. Competing diagrams involving New Physics (NP) phenomena may significantly affect the total amplitude and the Lorentz structure of the decay. These properties may be accessed through measurement of the branching fraction $\mathcal{B}$ or through an angular analysis. New results are presented using a data sample with an integrated luminosity of $\sim 1\,\text{fb}^{-1}$ collected in 2011 with the LHCb detector.

The presented results comprise: the worlds most precise measurement of angular observables in $B^0 \to K^{*0}\mu^+\mu^-$, including the worlds first measurement of q_0^2 [1]; the worlds best measurements of the $B^0 \to K^{*0}\mu^+\mu^-$ [1] and $B_s^0 \to \phi\mu^+\mu^-$ [2] partial branching fractions; the worlds first measurement of the $B^+ \to \pi^+\mu^+\mu^-$ total branching fraction [3]; the worlds first limits on $B \to \mu^+\mu^-\mu^+\mu^-$ [4] and the worlds best limits on $B \to \mu^+\mu^-$ [5] and $D^0 \to \mu^+\mu^-$ [6].

2 The angular analysis of $B^0 \to K^{*0}\mu^+\mu^-$

The angular distribution of the decay $B^0 \to K^{*0}\mu^+\mu^-$ may be parameterised by 6 complex amplitudes. These may be combined to form theoretically clean and experimentally accessible angular observables; F_L, the fraction of K^{*0} longitudinal polarisation; A_FB, the forward-backward asymmetry of the dimuon system; $S_3 = A_\text{T}^2(1 - F_\text{L})/2$, where A_T^2 is the asymmetry in the K^{*0} transverse polarisation [7,8]; A_IM, a T-odd CP asymmetry. These observables allow separation between the SM and a variety of NP models. The results of this analysis and the SM theory prediction [9] are shown in Fig. 1 [1]. No significant deviation from the SM theory prediction is observed.

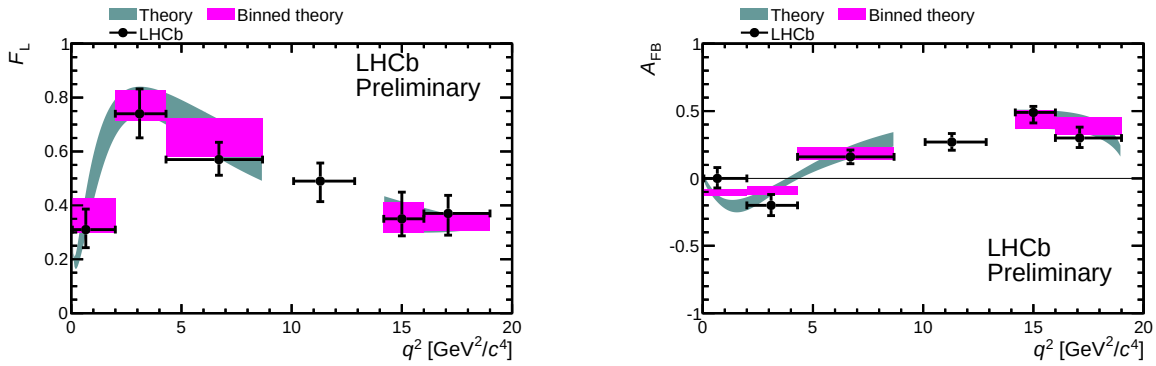

(a) $F_{\rm L}$

(b) $A_{\rm FB}$

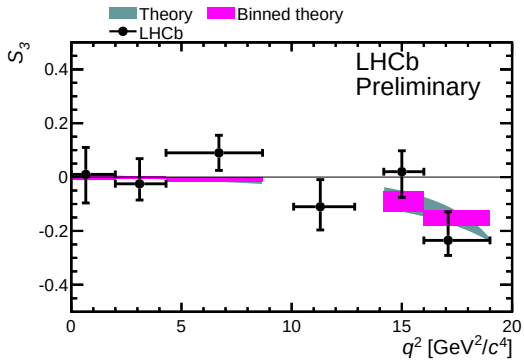

(c) S_3

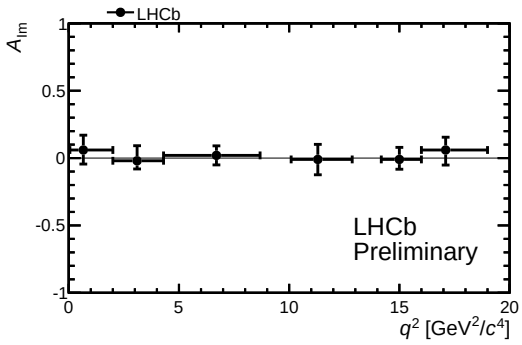

(d) $A_{\rm IM}$

Figure 1: $B^0 \to K^{*0}\mu^+\mu^-$ angular analysis results. Black points are results of a fit to the data sample. The error bars include both statistical and systematic uncertainties. The SM theory prediction is shown as a continuous band (grey) and binned according to the experimental binning scheme (pink) [9]. In (d) the SM theory prediction is close to zero. No significant deviation from the SM theory prediction is observed.

In the SM, the $A_{\rm FB}$ observable changes sign at a well defined point in q^2 that is largely free from form-factor uncertainties. This zero-crossing point q_0^2 was measured to be $q_0^2 = 4.9^{+1.1}_{-1.3}$ GeV$^2/c^4$ [1]. This is consistent with a the available SM theoretical predictions [9,10,11].

3 Branching fraction of $b \to \{s,d\}\mu^+\mu^-$ decays

3.1 Partial Branching Fraction of the Decays $B^0 \to K^{*0}\mu^+\mu^-$ and $B_s^0 \to \phi\mu^+\mu^-$

The $B^0 \to K^{*0}\mu^+\mu^-$ partial branching fraction measurement and SM theory prediction [9] is presented in Fig. 2b [1]. No significant deviation from the SM prediction is observed.

The theoretical estimate for the $B_s^0 \to \phi\mu^+\mu^-$ branching fraction is 1.61×10^{-6} [12]. The total branching fraction was extracted by normalising to $B_s^0 \to J/\psi\,\phi$ events, and was measured to be $(0.78 \pm 0.10(\text{stat}) \pm 0.06(\text{syst}) \pm 0.28(\mathcal{B})) \times 10^{-6}$, where the third error is due to the uncertainty on $\mathcal{B}(B_s^0 \to J/\psi\,\phi)$. The $B_s^0 \to \phi\mu^+\mu^-$ partial branching fraction is presented in Fig. 2a [2]. No significant deviation from the SM prediction is observed.

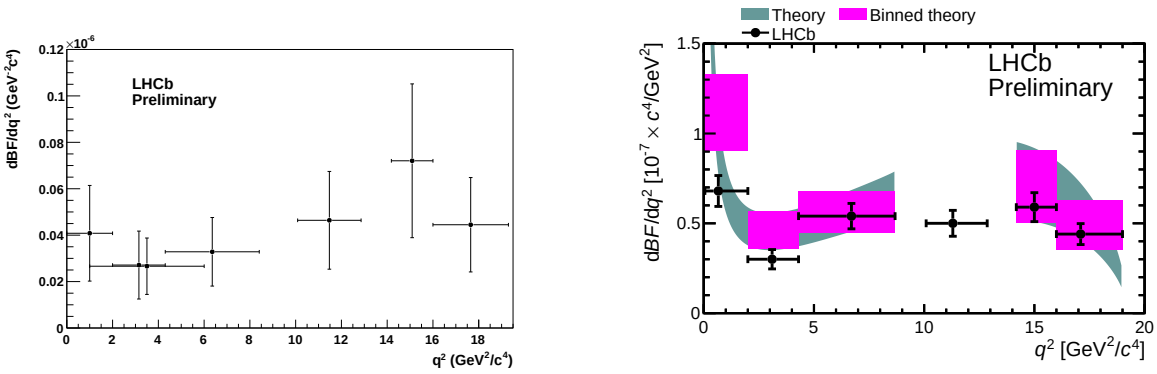

(a) (b)

Figure 2: Results of the $B_s^0 \to \phi\mu^+\mu^-$ (a) and $B^0 \to K^{*0}\mu^+\mu^-$ (b) partial branching fraction measurements. The error bars include both statistical and systematic uncertainties. In (b), the SM theory prediction is shown as a continuous band (grey) and binned according to the experimental binning scheme (pink). No significant deviation from the SM theory prediction is observed.

3.2 Total brancing fraction of the decay $B^+ \to \pi^+\mu^+\mu^-$

Unlike $b \to s\ell^+\ell^-$ transitions, no $b \to d\ell^+\ell^-$ has previously been observed. In the SM $B^+ \to \pi^+\mu^+\mu^-$ decays are suppressed with respect to $B^+ \to K^+\mu^+\mu^-$ decays by a factor of ~ 25, from the ratio of the CKM elements $|V_{td}|/|V_{ts}|$. The theoretical estimate for the total branching fraction in the SM is $(1.96 \pm 0.21) \times 10^{-8}$ [13]. The distribution of $B^+ \to \pi^+\mu^+\mu^-$ candidates observed in data is presented in Fig. 3. The measured branching fraction is $2.4 \pm 0.6\,(\text{stat}) \pm 0.2\,(\text{syst})) \times 10^{-8}$. This is consistent with the SM theory prediction and is the first observation of the $B^+ \to \pi^+\mu^+\mu^-$ decay; the rarest B decay ever observed [3].

4 Branching fraction of purely leptonic B^0 and D^0 decays

4.1 New limits on the decay $B \to \mu^+\mu^-\mu^+\mu^-$

The dominant contribution for a B meson decaying to a four muon final state comes from the decay $B_s^0 \to J/\psi\,\phi$ with both the J/ψ and ϕ decaying into two muons. The branching fraction estimate for this process is $(2.3 \pm 0.9) \times 10^{-8}$ [14]. The combined branching fraction from other sources is expected to be $< 10^{-10}$ [15 16]. This can be significantly enhanced in NP models through FCNC processes mediated by new particles that decay into $\mu^+\mu^-$ pairs. The distribution of $B \to \mu^+\mu^-\mu^+\mu^-$ candidates observed in data, after J/ψ and ϕ vetoes are applied, is presented in Fig. 4. The observed events are consistent with the expectation from background. A branching fraction limit was set at $< 5.4 \times 10^{-9}$ and $< 1.3 \times 10^{-8}$ at 95% C.L. for the B^0 and B_s^0 mode respectively [4]. These limits are consistent with the SM theory predictions.

4.2 Improved limits on the decay $B \to \mu^+\mu^-$ and $D^0 \to \mu^+\mu^-$

The decays of B mesons to muon pair final states are highly suppressed in the SM. Theoretical predictions for the branching fractions for $B \to \mu^+\mu^-$ decays are $(3.2 \pm 0.2) \times 10^{-9}$ [17] and $(0.10 \pm 0.01) \times 10^{-9}$ [18] for the B_s^0 and B^0 decays respectively. Improved branching fraction limits were set at $< 4.5 \times 10^{-9}$ and 1.03×10^{-9} at 95% C.L. respectively [5]. These limits are consistent with the SM theory predictions.

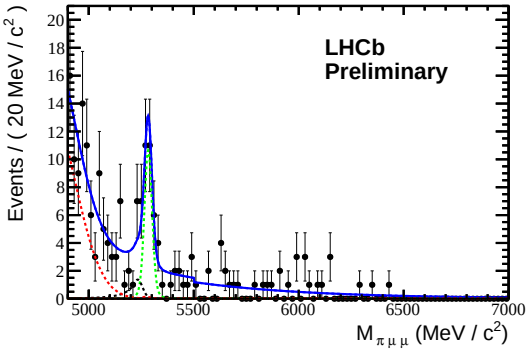

Figure 3: The $\pi^+\mu^+\mu^-$ invariant mass distribution of $B^+ \to \pi^+\mu^+\mu^-$ candidates in the data. The fitted shape (solid blue) comprises signal (green dash), background (red dash) and $B^+ \to K^+\mu^+\mu^-$ (black dash) components.

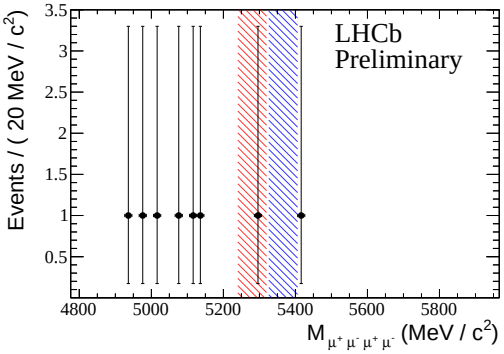

Figure 4: The $\mu^+\mu^-\mu^+\mu^-$ invariant mass distribution of $B \to \mu^+\mu^-\mu^+\mu^-$ candidates in the data. The B^0 (red striped) and B_s^0 (blue striped) search regions are indicated.

The branching fraction of the $D^0 \to \mu^+\mu^-$ is dominated by long distance contributions; the SM theory prediction has an upper limit of 6×10^{-11} at 90% C.L. [19]. The best experimental limit was previously set by BELLE at $< 1.4 \times 10^{-7}$ at 90% C.L. [20]. Improved experimental limits were set at $< 1.3 \times 10^{-8}$ at 95% C.L. using $\sim 0.9\,\text{fb}^{-1}$ of integrated luminosity. This is consistent with the SM theory prediction and improves the current world best limit by more than an order of magnitude.

References

1. LHCb Collaboration, CERN-LHCb-CONF-2012-008 (2012).
2. LHCb Collaboration, CERN-LHCb-CONF-2012-003 (2012).
3. LHCb Collaboration, CERN-LHCb-CONF-2012-006 (2012).
4. LHCb Collaboration, CERN-LHCb-CONF-2012-010 (2012).
5. LHCb Collaboration, CERN-PH-EP-2012-072 (2012).
6. LHCb Collaboration, CERN-LHCb-CONF-2012-005 (2012).
7. F. Kruger *et al*, Phys. Rev. **D71**, 094009 (2005).
8. W. Altmannshofer *et al*, JHEP **01**, 019 (2009).
9. C. Bobeth *et al*, JHEP **07**, 067 (2011).
10. M. Beneke *et al*, Eur. Phys. J. **C41**, 173-188 (2005).
11. A. Ali *et al*, Eur. Phys. J. **C47**, 625-641 (2006).
12. C.Q. Geng *et al*, J. Phys. G **G29**, 1103-1118 (2003).
13. S. Hai-Zhen *et al*, Commun. Theor. Phys. **50**, 696 (2008).
14. K. Nakamura et al. (Particle Data Group), J. Phys. G **37**, 075021 (2010).
15. D. Melikhov *et al*, Phys. Rev. **D70**, 114028 (2004).
16. D. Melikhov *et al*, Phys. At. Nucl. **68**, 1842 (2005).
17. A. J. Buras *et al*, JHEP **10**, 009 (2010).
18. A. J. Buras, Acta Phys. Polon. **B41**, 2487-2561 (2010).
19. G. Buchalla *et al*, Rev. Mod. Phys. **68**, 1125-1144 (1996).
20. BELLE Collaboration, Phys. Rev. **D81**, 091102 (2010).